

Competitive Sorption Behavior of Arsenic, Selenium, Copper and Lead by Soil and Biosolid Nano- and Macro-Colloid Particles

Jessique Ghezzi, Anastasios Karathanasis, Chris Matocha, Jason Unrine, Yvonne Thompson

Department of Plant and Soil Sciences, University of Kentucky, Lexington, KY, USA
Email: akaratha@uky.edu

Received 15 July 2014; revised 12 August 2014; accepted 30 August 2014

Copyright © 2014 by authors and Scientific Research Publishing Inc.
This work is licensed under the Creative Commons Attribution International License (CC BY).
<http://creativecommons.org/licenses/by/4.0/>



Open Access

Abstract

Limited information exists on natural nanocolloid sorption behavior of As, Se, Cu and Pb in the environment. They are expected to have variable competitive sorption characteristics depending on size and composition and may transport elevated contaminant loads into surface and ground waters. A comprehensive characterization of their interactions with contaminants could provide a better understanding of the risks they pose to the environment. This study evaluated the sorption behavior of soil and biosolid nano- and macro-colloids with different mineralogical compositions for As, Se, Cu, and Pb contaminants. Single- and multi-contaminant Freundlich isotherms were used to evaluate sorption affinity for the contaminants among the different colloid sizes and compositions. Sorption trends based on size indicated greater affinity for As and Cu by the smectitic and kaolinitic nanocolloids, greater affinity for Pb by the kaolinitic nanocolloids, and greater affinity for As, Se and Pb by bio-nanocolloids over corresponding macrocolloid fractions. Both, single- and multi-contaminant isotherms indicated sorption preferences for cation over anion contaminants, but with somewhat contrasting sequences depending on size and composition. Multi-contaminant isotherms generally predicted greater sorption affinities likely due to bridging effects, particularly for anionic contaminants. Surface properties such as zeta potentials, cation exchange capacity (CEC), surface area (SA), organic carbon (OC), and OC:SA significantly but variably affected sorption characteristics among the differing colloid sizes and compositions. Colloid zeta potential and pH shifts in the presence of different contaminant loads suggested prevalence of inner sphere bonding mechanisms for sorption of cation contaminants by mineral colloids and outer sphere sorption for cation and anion contaminants by bio-colloids.

Keywords

Sorption Affinity, Single-Contaminant Isotherms, Multi-Contaminant Isotherms, Size Effects,

Composition Effects

1. Introduction

Major environmental concerns have developed within the past decade in regard to large-scale contamination of natural resources. The vast devastation experienced from catastrophic events such as hurricanes Sandy (2012) and Katrina (2005) have highlighted an ongoing water quality issue, which is the transport or mass influx of contaminants into groundwater supplies following storm events. Remediators need information on contaminant interactions at the soil-water interface and how these interactions affect contaminant plume movement and contaminant transport in surface and ground waters. One potential vector of contaminant transport that should be further investigated is that of naturally occurring environmental nanoparticles, such as those derived from soils or biosolids [1]-[4]. Soil nanoparticles include humic substances, clay minerals/colloids, and metal hydroxides [4]-[6]. Large volumes of biosolid nanoparticles are introduced into the environment from human and animal wastes applied to land as fertilizers [7]. More recently, the development and application of engineered nanoparticles for remediation of contaminant plumes has also raised concerns about their mobility and biotoxicity in the environment [8] [9]. Research on naturally occurring environmental nanoparticles is limited with regard to their behavior in environmental media, both as potential contaminant transport vectors and as models for manufactured nanoparticles [1]-[4] [10].

Current findings suggest that soil and biosolid nanocolloids may possess larger surface area and increased reactivity than macrocolloid fractions and therefore, a greater potential to sorb and transport larger quantities of heavy metals to groundwater [3] [5] [11]. Both mineral and biosolid-derived nanocolloids can form inner- and outer-sphere complexes with heavy metals via surface siloxane, aluminol, carboxylic, and phenolic groups [12] [13]. Drops in pH or zeta potential with increasing contaminant loads have been associated with inner sphere sorption due to proton release after the exchange of the cation contaminant, or due to hydrolysis/precipitation of the metals [14]. The type of bonding between nanocolloid surfaces and contaminants also dictates the likelihood of re-suspension of the contaminant in different ionic or pH environments, further demonstrating the need for a better understanding of the solid-solution interface reactions between nanocolloids and potential contaminants [11] [12].

Elevated concentrations of contaminants such as As, Se, Cu, and Pb in water supplies have raised considerable environmental concerns [12] [13]. Increased levels of these contaminants are attributed to both soluble and particulate sources [5] [11]. Both As and Se are considered as metalloids, and are usually present as oxy-anions in soil environments while Cu and Pb are cationic metals [15] [16]. Studies of their interactions with various clay minerals suggest that their sorption behavior is controlled by the competition between ions in solution and the clay surface, pH, ionic strength, and mineralogy [12] [17]. Arsenic and Se tend to form outer sphere complexes with variable charge minerals and phyllosilicate edges and inner sphere complexes directly with Fe-oxyhydroxides or through bridging with Fe/Al hydrolytic species associated with organic functional groups [18] [19]. On the other hand, the interaction of Cu and Pb with colloids is mainly controlled by ion exchange processes, with electrostatic surface bonding and chemisorption to surface SiOH and AlOH groups [19]. Since most phyllosilicate mineral surfaces are negatively charged, they are expected to repel oxy-anions like As and Se, and attract cations such as Cu and Pb. However, the presence of organic functional groups and/or Fe/Al-oxyhydroxides as discrete phases or coatings on clay surfaces may cause significant surface charge alterations and drastic contaminant sorption behavior changes in colloidal fractions albeit with their mineralogical composition [20]-[22]. While the sorption behavior of As, Se, Cu, and Pb contaminants with clay sized fractions of different mineralogical composition has been extensively studied, very little information exists on their interactions with nano-sized particles under single- and multi-contaminant solution environments.

The objectives of this study were to evaluate the sorption affinity of soil and biosolid nano- and macro-colloids of diverse composition for As, Se, Cu, and Pb under single- and multi-contaminant solution environments.

2. Methods and Materials

2.1. Colloid Generation

The Bt horizons of three Kentucky soils of differing mineralogy were used to generate the mineral colloids: Ca-

least-variant (fine, smectitic, mesic mollic Hapludalf), Tilsit (fine-silty, mixed, mesic Typic Fragiudult), and Trimble (fine-loamy, siliceous, mesic Typic Paleudult), referred to herein as smectitic, mixed, and kaolinitic, respectively. Biosolid colloids were fractionated from an aerobically digested municipal sewage sludge obtained from Jessamine County, Kentucky. Centrifuge fractionations using Stokes law allowed separation of the two size classes (nanocolloids < 100 nm and macrocolloids 100 - 2000 nm) using a Centra GP8R Model 120 centrifuge (Thermo IEC). Clay fractions were separated from bulk soils by centrifugation at 107 RCF for 3.5 minutes, as calculated using a rotor radius of 170 mm, 107 RCF, a density difference of $1650 \text{ kg}\cdot\text{m}^{-3}$, and viscosity of 0.0008904 Pas . Nanocolloids were then separated from corresponding macrocolloids at 4387 RCF for 46 minutes, as calculated using a rotor radius of 170 mm, a speed of 4387 RCF, a density difference from water of $1650 \text{ kg}\cdot\text{m}^{-3}$, and viscosity of 0.0008904 Pas [5] [23]. The colloids were generated with de-ionized water (resistivity of $1 \mu\Omega\cdot\text{cm}$ at 25°C).

2.2. Sorption Isotherms

Nano- and macro-colloid affinities for the four contaminants were evaluated with single- and multi-contaminant adsorption isotherms using duplicate colloid suspensions of $50 \text{ mg colloid L}^{-1}$ in de-ionized water spiked with 0, 0.2, 0.5, 1, 2, 5 and $10 \text{ mg}\cdot\text{L}^{-1}$ of As, Se, Cu, and Pb. Equilibrium aqueous solutions of Pb, Cu, As and Se were prepared from PbCl_2 (98% purity, Aldrich Chemicals, Milwaukee, WI), CuCl_2 (>99% purity, Sigma Chemical Company, St. Louis, MO), arsenic acid $\text{Na}_2\text{HAsO}_4\cdot 7\text{H}_2\text{O}$ (98% purity, Sigma Chemical Company, St. Louis, MO), and sodium selenate decahydrate $\text{Na}_2\text{SeO}_4\cdot 10\text{H}_2\text{O}$ (99.9% purity, Sigma Chemical Company, St. Louis, MO). Multi-contaminant adsorption isotherms were generated with multi-contaminant equilibrium solutions in which the sum of the four contaminant concentrations was 0, 0.2, 0.5, 1, 2, 5, and 10 mg , respectively. MINEQL⁺ speciation of the equilibrium solutions suggested the following predominant species: 99.9% Pb^{2+} , 99.9% Cu^{2+} , 99.7% SeO_4^{2-} (selenate, VI), and 98.6% AsO_4^{3-} (arsenate, V). Isotherm samples were equilibrated by shaking for 24 hours at room temperature (25°C) in polyethylene tubes with pH measurements taken at 0 and at 24 hours. After shaking, $0.025 \mu\text{m}$ nitrocellulose filters were used to separate the supernatant from the colloidal fraction. Supernatant fractions were preserved with 1% nitric acid, stored in polyethylene vials, and analyzed within 24 hours via inductively coupled plasma mass spectroscopy (ICP-MS). The mass of contaminant sorbed per mass of colloid was calculated and plotted using the Freundlich equation:

$$q = \frac{V \times (C_{in} - C_o)}{M} = \mu\text{mol} \cdot \text{kg}^{-1},$$

where q is the mass of contaminant sorbed per mass of colloid, V is the solution volume used in the sorption isotherm experiment, C_{in} is the amount of contaminant added in solution, C_o is the amount of contaminant measured at equilibrium and M is the mass of the sorbent. The log version of this equation ($\text{Log}q = N\text{Log}C_{eq} + \text{Log}K_f$), yields a straight line with N slope, $\text{Log}C_{eq}$ the x-variable and $\text{Log}K_f$ (Freundlich sorption coefficient) the y-intercept [24]. Isotherms were also normalized for colloid surface area and OC content but did not produce statistically significant trends [25].

2.3. Physico-Chemical and Surface Characterizations

All analyses were performed on suspensions of $50 \text{ mg colloid L}^{-1}$ in de-ionized water. A Malvern Instruments Zetasizer Nano ZS (Malvern, United Kingdom) measured suspensions for intensity weighted mean particle hydrodynamic diameters (z-average diameter) using dynamic light scattering (173° backscatter analysis method). Nano- and macro-colloid crystallite sizes were determined using transmission electron microscopy (TEM; JEOL 2010F, Tokyo, Japan) and scanning electron microscopy (SEM; Hitachi S-4300, Tokyo, Japan), respectively. ImageJ software was used to calculate average minimum diameters (ImageJ 1.46r, Wayne Rasband, National Institutes of Health, USA). Surface area was measured using the Ethylene Glycol Monoethyl Ether (EGME) method. Electrical conductivity and pH were measured on a Denver Instruments Model 250 pH*ISE*electrical conductivity meter (Arvada, CO). Cation exchange capacity was determined using an adapted version of the ammonium acetate method and reported as a sum of the base cations Ca^{2+} , Mg^{2+} , K^+ , and Na^+ , as measured with a Varian Spectr AA 50B atomic absorption spectrometer. Organic carbon was measured on a Flash EA 1112 Series NC Soil Analyzer (Thermo Electron Corporation) with a Mettler Toledo MX5 microbalance. Zeta potentials in the presence of 0 and $2 \text{ mg}\cdot\text{L}^{-1}$ Pb, Cu, As, and Se were converted from electrophoretic mobility measure-

ments using the Smoluchowski approximation on a Malvern Zetasizer Nano ZS (Malvern, United Kingdom).

2.4. Mineralogical Characterization

Mineralogical characterizations were completed using X-ray diffraction (XRD) and Thermogravimetric analysis (TG) on a Phillips PW 1840 diffractometer and PW 1729 X-ray generator (Mahwah, NJ), and a Thermal Analyst 2000 (TA Instruments) equipped with a 951 Thermogravimetric Analyzer (DuPont Instruments), respectively [23].

2.5. Statistical Analysis

The standard accepted error level for all duplicate and triplicate samples was 15%. Mean differences in sorption Freundlich coefficients ($\text{Log}K_f$) and changes in the isotherm pH were calculated using the general linear model (PROC GLM). Mean differences (overall and based on mineralogy, size, and contaminant) were developed using Fisher's protected least significant difference test (LSD) in SAS using probability levels of 0.05, unless otherwise noted. Competitive sorption relationships were analyzed between colloid properties and sorption coefficients using multiple regression analysis with probability levels of $\alpha < 0.05$ and $\alpha < 0.01$ in SAS 9.3 (SAS Institute Inc., Cary, NC, USA).

3. Results and Discussion

3.1. Single-Contaminant Isotherms

The data conformed well to the Freundlich equation, showing R^2 values between 0.93 and 0.99 with differing sorption trends for each contaminant. The majority of $1/n$ values were < 1.0 , suggesting uniform sorption surface coverage, but As sorption by biosolid colloids and Se sorption by smectitic colloids indicated the potential for multiple coverage mechanisms with $1/n$ values > 1.0 . Generally, As sorption coefficients were the lowest among the contaminants studied (Figure 1). Macrocolloid sorption affinities for As ranged from 1.67 to 3.48, with the highest representing the mixed mineralogy and the lowest the biosolid colloids (Figure 1). Sorption affinities for As within the nanocolloids ranged from 1.85 to 3.60, with the highest affinity associated with the kaolinitic and the lowest with the biosolid colloids (Figure 1). Statistically significant trends among compositions for As affinity by macrocolloids followed the sequence: Mixed (A) $>$ Smectitic (B) $>$ Kaolinitic (C) $>$ Biosolid (D); and by nanocolloids Kaolinitic (A) $>$ Smectitic (B) $>$ Mixed (C) $>$ Biosolid (D) ($\alpha < 0.05$). Typically, Fe-oxy-hydroxides and kaolinitic clays have demonstrated higher sorption capacities for arsenate [26] [27] than for illite or smectite [19], especially in the presence of humic acid surface coatings [21]. However, Fe-hydroxide and organic coatings may increase As sorption by phyllosilicate minerals via inner sphere complex formation [18] [19]. The biosolid colloids showed lower overall As affinity than the mineral colloids (Figure 1), contrary to studies showing increased arsenate sorption with increasing organic matter composition [21] [27]. This could be explained by the higher pH (Table 1) and phosphate content of the bio-colloids compared to the mineral colloids. Arsenate sorption has been shown to decrease with increasing pH and phosphate has a tendency to displace As [18] [28]. A colloid size comparison for As affinity suggested greater sorption for nano-colloids than macro-colloids in all compositions, except for the mixed colloids ($\alpha < 0.05$; Figure 1). Ideally, the nano-fractions due to their higher negative zeta potentials (Table 2) were expected to have lower K_f values for anionic contaminants, but the presence of OC surface coatings and bridging effects with Fe/Al hydrolytic species (Table 1) may have enhanced their affinity for As [19] [29].

Selenium also exhibited low sorption coefficients compared to those of Cu and Pb (Figure 1). Sorption affinities for Se within the macrocolloids showed no particular preference for composition, ranging from 3.09 to 3.49. The highest affinity was observed with the mixed mineralogy and the lowest with the smectitic colloids (Figure 1). The wider range was observed within the nanocolloids (2.06 to 3.53) with the highest affinity represented by the mixed mineralogy and the lowest the smectitic composition (Figure 1). The higher affinity of the mixed colloids for Se over the smectitic could be associated with contributions from its higher kaolinite content and from the mica minerals that exhibit similar to kaolinite Se sorption trends at low pH (Table 1) [30] [31]. Statistically significant sorption affinity for Se by macrocolloids followed the sequence: Mixed (A) $>$ Kaolinitic = Biosolid (B) $>$ Smectitic (C); and by nanocolloids Mixed (A) $>$ Biosolid (B) $>$ Kaolinitic (C) $>$ Smectitic (D) ($\alpha < 0.05$; Figure 1). Negative linear correlations between Se sorption affinity and smectite content are consistent

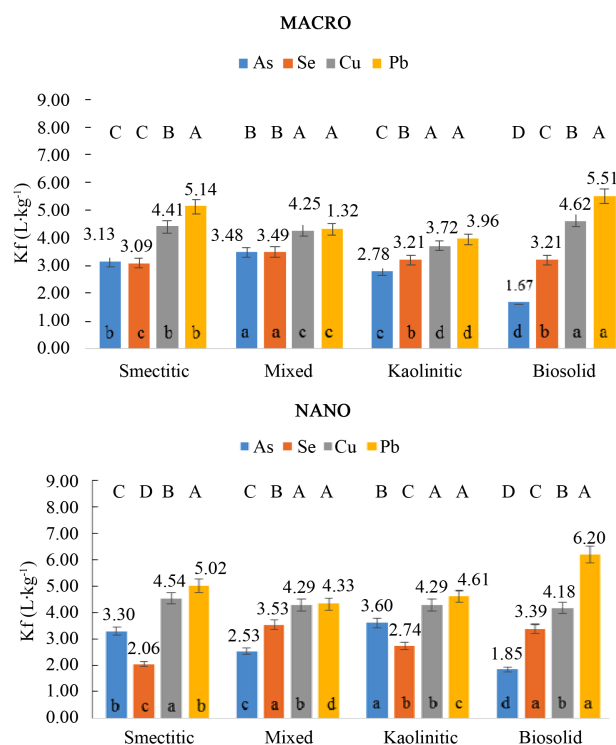


Figure 1. Single-contaminant isotherm Kf values for As, Se, Cu, and Pb for macro- and nano-colloid fractions of different composition (capital letters portray trends across all four contaminants within each composition, while lower case letters display trends for each contaminant across all four compositions).

Table 1. Selected physical and chemical characteristics of nano- and macro-colloid fractions.

Size Fraction	Colloid Composition							
	Smectitic		Mixed		Kaolinitic		Biosolid	
	Macro	Nano	Macro	Nano	Macro	Nano	Macro	Nano
DLS [†] Mean Hydrodynamic Diameter (d _h) ±SD [‡] (nm)	487 ± 10	181 ± 3	596 ± 21	205 ± 4	545 ± 25	187 ± 4	4456 ± 599	353 ± 8
SEM/TEM [§] Mean Smallest Particle Size ±SD [‡] (nm)	328 ± 144	37 ± 13	549 ± 394	7 ± 5	288 ± 184	41 ± 19	363 ± 338	50 ± 19
Surface Area (SA, m ² ·g ⁻¹) ±SD [‡]	708 ± 137	879 ± 76	420 ± 105	466 ± 10	333 ± 37	389 ± 44	1674 ± 70	1303 ± 63
Ionic Strength (IS, mol·L ⁻¹) [§]	4.99 × 10 ⁻⁵	7.71 × 10 ⁻⁵	3.70 × 10 ⁻⁵	3.92 × 10 ⁻⁴	3.64 × 10 ⁻⁵	4.83 × 10 ⁻⁵	1.97 × 10 ⁻⁴	5.96 × 10 ⁻⁴
Natural pH	4.92	5.12	5.07	4.92	4.91	5.38	5.39	5.25
CEC (cmol _c ·kg ⁻¹) [#]	35.0 ± 12.8	42.2 ± 15.1	8.9 ± 1.6	10.5 ± 1.7	6.9 ± 1.8	13.1 ± 2.8	37.6 ± 14.8	71.0 ± 23.0
OC (mg·kg ⁻¹) ^{**}	658	897	645	774	430	647	1300	16000
OC:SA	0.93	1.02	1.54	1.66	1.29	1.66	0.78	12.28
Mineralogy (%) [*]	K ₂₉ , Ge ₇ , Q ₆ , M ₁₀ , Sm ₄₈	K ₃₀ , Ge ₉ , Q ₄ , M ₆ , Sm ₅₁	K ₄₂ , Ge ₅ , Q ₅ , MVI ₇ , M ₃₁ , HIV ₁₀	K ₄₆ , Ge ₇ , Q ₃ , M ₃₀ , MVI ₇ , HIV ₇	K ₅₂ , Ge ₁₂ , Gi ₅ , Q ₄ , M ₃ , HIV ₂₄	K ₅₅ , Ge ₁₅ , Gi ₆ , Q ₂ , M ₃ , HIV ₁₉	NA	NA

[†]DLS = Mean intensity weighted hydrodynamic diameter (d_h) determined by Dynamic Light Scattering. [‡]SD = Standard Deviation of duplicate or triplicate measurements. [§]Ionic Strength (IS) = 0.0127 × Electrical Conductivity (millimhos·cm⁻¹). [¶]SEM = Scanning Electron Microscopy, TEM = Transmission Electron Microscopy. [#]CEC = Cation Exchange Capacity by sum of cations. ^{**}OC = Total Organic Carbon-Dissolved Organic Carbon (inorganic carbon contributions were assumed to be 0 due to low pH). ^{*}Mineralogy (K = Kaolinite, Ge = Geothite, Gi = Gibbsite, Q = Quartz, M = Mica, Sm = Smectite, MVI = Mica-Vermiculite Interstratified, HIV = Hydroxy-Interlayered Vermiculite, NA = Not Applicable).

Table 2. Zeta potential and pH for macro- and nano-colloid fractions of different composition in the absence and in the presence of equal amounts of As, Se, Cu, and Pb, totaling 0, 2 and 10 mg·L⁻¹.

Colloid Composition	Colloid Size Fraction			
	Macro		Nano	
	Zeta potential with 0, 2, and 10 mg/L contaminant additions (mV)	pH with 0, 2, and 10 mg/L contaminant additions	Zeta potential with 0, 2, and 10 mg/L contaminant additions (mV)	pH with 0, 2, and 10 mg/L contaminant additions
Smectitic	-27, -18, -11	4.60, 4.67, 4.38	-28, -25, -18	5.11, 5.02, 4.56
Mixed	-34, -29, -26	5.50, 4.45, 4.24	-39, -38, -22	4.84, 4.61, 4.33
Kaolinitic	-34, -30, -26	4.98, 4.96, 4.40	-38, -31, -26	4.90, 4.79, 4.55
Biosolid	-19, -21, -25	5.11, 5.42, 5.18	-11, -24, -29	5.25, 5.79, 5.69

with the anionic behavior of this contaminant ($R^2 = -0.42^*$) [30]. Additionally, the Se affinity of kaolinite may have been enhanced by contributions from goethite and gibbsite (Table 1) through formation of inner- and outer-sphere complexes [32] [33]. With the exception of the mixed colloids, Se sorption affinity was influenced by size, showing greater sorption by the smectitic and kaolinitic macro-fraction and an opposite trend by the bio-colloid nano-fraction (Figure 1). Higher macrocolloid affinity for this anionic contaminant can be probably attributed to the lower pH of the smectitic and kaolinitic macro-fractions (Table 1) and the increased repulsion of Se by the nanocolloids due to more negative surface charge induced by OC surface coatings (Table 1 and Table 2) [13] [20]. In contrast, the bio-colloids exhibited greater sorption affinity for Se in the nano-fraction—most likely due to the lower pH as was the case with As in spite of higher surface charge, OC, and OC:SA ratios (Figure 1, Table 1 and Table 2). The bio-colloid (macro- and nano-fractions) sorption affinity for Se was significantly higher than that for As (Figure 1; $\alpha < 0.05$) in spite of the lower shared charge [34] in agreement with other findings in waste-amended soils [35].

As would be expected for cationic contaminants, Cu sorption affinity was significantly higher than As and Se in all colloid fractions (Figure 1; $\alpha < 0.05$). Sorption coefficients within the macro-fractions ranged from 3.72 to 4.62, with the highest affinity representing the biosolid composition and the lowest the kaolinitic (Figure 1). Copper has been shown to dominantly associate with mineralizable biosolid fractions [36], forming multi-ligand complexes with a variety of organic surface functional groups [19]. In contrast, within the nanocolloid fractions, the highest affinity was associated with the smectitic (4.54) and the lowest (4.18) with the biosolid composition (Figure 1). Statistically significant differences for Cu sorption affinity within the macrocolloids followed the sequence: Biosolid (A) > Smectitic (B) > Mixed (C) > Kaolinitic (D); and for the nanocolloid fraction: Smectitic (A) > Mixed = Kaolinitic (B) > Biosolid (C) ($\alpha < 0.05$; Figure 1). The differing trends for Cu sorption affinity observed in the biosolid macro- vs. nano-fractions may be explained by the greater OC:SA ratios of the bio-nanocolloids that could potentially induce aggregation and block surface sorption surface sites or by the presence of less reactive organic functional groups (Table 1). This is corroborated by the lower initial zeta potential values of the biocolloid nano-fractions (Table 2). In addition, the lower pH maintained by the biosolid macrocolloids compared to the nanocolloid fractions after the addition of different Cu concentrations may have enhanced dissociation and surface organic complexation reactions [37] [38]. Other than the biocolloids, statistically greater Cu sorption affinity based on size was also demonstrated by the kaolinitic and smectitic nanocolloids over the macrocolloids (Figure 1; $\alpha < 0.05$). The greater cation sorption affinities of these nanocolloids are likely due to higher negative zeta potentials and greater surface area as compared to that of the macrocolloids (Table 1 and Table 2). There were no significant differences in sorption of Cu based on size for the mixed colloids (Figure 1).

Sorption affinities for Pb were the highest compared to other contaminants. Within the macrocolloids the highest coefficient (5.51) was associated with the biosolid composition and the lowest (3.96) with the kaolinitic (Figure 1). Within the nanocolloids Kf values for Pb ranged from 4.33 to 6.20, with the highest value representing the biosolid composition and the lowest the mixed (Figure 1). Based on composition, macrocolloid affinity for Pb followed the sequence: Biosolid (A) > Smectitic (B) > Mixed (C) > Kaolinitic (D); and Biosolid (A) > Smectitic (B) > Kaolinitic (C) > Mixed (D) for nanocolloids ($\alpha = 0.05$). These trends are comparable to those reported elsewhere, indicating preferential sorption of Pb by biosolids over other cation metals like Cu or

Zn [23]. The greater cation sorption affinities of the nanocolloids are likely due to greater attraction of cation contaminants to their higher negative zeta potentials and greater surface area availability for sorption as compared to that of the macrocolloids (Table 1 and Table 2). Increased affinity for Pb by smectitic minerals has been attributed to their high permanent charge and ability to form inner sphere complexes with exposed surface –OH groups [19] [39]. Only the kaolinitic and biosolid colloids showed size sorption preferences, with the nano-fractions exhibiting greater K_f values than the macro-size fractions, apparently due to higher CEC, SA and OC content. Statistical correlations (R^2 , $\alpha < 0.05$) of Pb sorption coefficients with the above parameters were 0.78, 0.92, and 0.56, respectively.

Single-contaminant isotherm data normalized by surface area and organic carbon did not provide significant differences from mass based isotherms in colloid size or composition trends. However, all isotherm normalization methods indicated preferential sorption of cation-(Cu, Pb) over anion-(As, Se) contaminants [12] [23] [25]. Overall, single-contaminant isotherms showed the following contaminant sorption preference: Pb (A) > Cu (B) > As (C) = Se (C) ($\alpha < 0.05$). Greater sorption of Pb over Cu is likely due to the lower hydrolysis constant of Pb [19] [22] [38]. The similar sorption affinities for As and Se contradict other findings showing preferential sorption of arsenate over selenate [34] but may be explained by the higher bio-colloid preference for Se, which has overshadowed the expected differences in anion sorption. Sorption trends based on colloid size varied, with the smectitic and kaolinitic nanocolloids demonstrating greater affinities for As and Cu contaminants than corresponding macrocolloid fractions, but showing opposite trends for Se. The kaolinitic nano-fraction indicated a greater affinity for Pb over the macro-fraction. The bio-nanocolloids showed greater affinity for As, Se, and Pb than for the corresponding macrocolloids, but showed the opposite trend for Cu. Finally, the mixed colloids exhibited size-based sorption trends only for As, showing greater affinity in the macro- than the nano-fraction (Figure 1; $\alpha < 0.05$).

Published research with relatively pure minerals suggests that kaolinitic clays typically have a greater affinity to sorb anions (including oxy-anions like Se and As) than illitic or smectitic clays [19]. Also, surface silanol and aluminol groups exposed on the interlayer surfaces of 2:1 minerals tend to preferentially sorb cation contaminants such as Cu and Pb [19]. The lack of consistent sorption differences by colloid size and even composition in this study may be explained by the diverse natural mixture of minerals present in each colloid fraction as well as the nature and extent of Fe, Al, and organic moieties coating their surfaces. It also demonstrates the unpredictable complexities of modeling contaminant sorption and transport behavior of natural environmental nano- and macro-colloidal fractions [5] [11] [33].

3.2. Multi-Contaminant Isotherms

Competition among As, Se, Cu and Pb sorption was established through multi-contaminant isotherms for each colloid-size fraction. The data conformed reasonably well to the Freundlich equation with lower R^2 values (0.84 ± 0.12) and more $1/n$ values >1 than the single contaminant sorption isotherms implying that multiple sorption mechanisms were triggered by the presence of all four contaminants. Multi-contaminant isotherm K_f values by colloid size and composition are shown in Figure 2. Overall, within the same composition multi-contaminant K_f values were significantly higher than single-contaminant K_f values for both sizes for all contaminants except As (Figure 1 and Figure 2). This is probably the result of bridging effects induced by anionic and cationic contaminants in the mixture. The mixed macro- and nano-colloid fractions indicated equal affinity of Pb and Cu, but greater affinity for Se than As (Figure 2). The kaolinitic and biosolid macrocolloids indicated preferential sorption for Pb over Cu, with no significant differences between the anionic contaminants (Figure 2). These trends are consistent with other findings indicating preferential sorption of Pb over Cu by kaolinite [22] and similar affinities for Cu and Pb by humic acid substances, and Fe/Mn-oxides [19]. Opposing trends were displayed by the smectitic macrocolloids and kaolinitic nanocolloids, portraying greater Cu sorption over Pb, and more affinity for Se than As (Figure 2). Finally, the smectitic and biosolid nanofractions shared the following sorption affinity sequence: Pb (A) > Cu (B) > Se (C) > As (D) (Figure 2).

Overall, counting all colloids, the multi-contaminant isotherms showed the following sorption preference trends: Pb (A) = Cu (A) > Se (B) > As (C) ($\alpha < 0.05$); with cation contaminants indicating more competitive sorption affinity compared to the anion contaminants as was the case with the single-contaminant isotherms (Figure 1 and Figure 2). However, two main differences are manifested in the similar sorption affinity for Cu and Pb compared to Pb > Cu and the greater affinity for Se over As compared to Se = As shown by the sin-

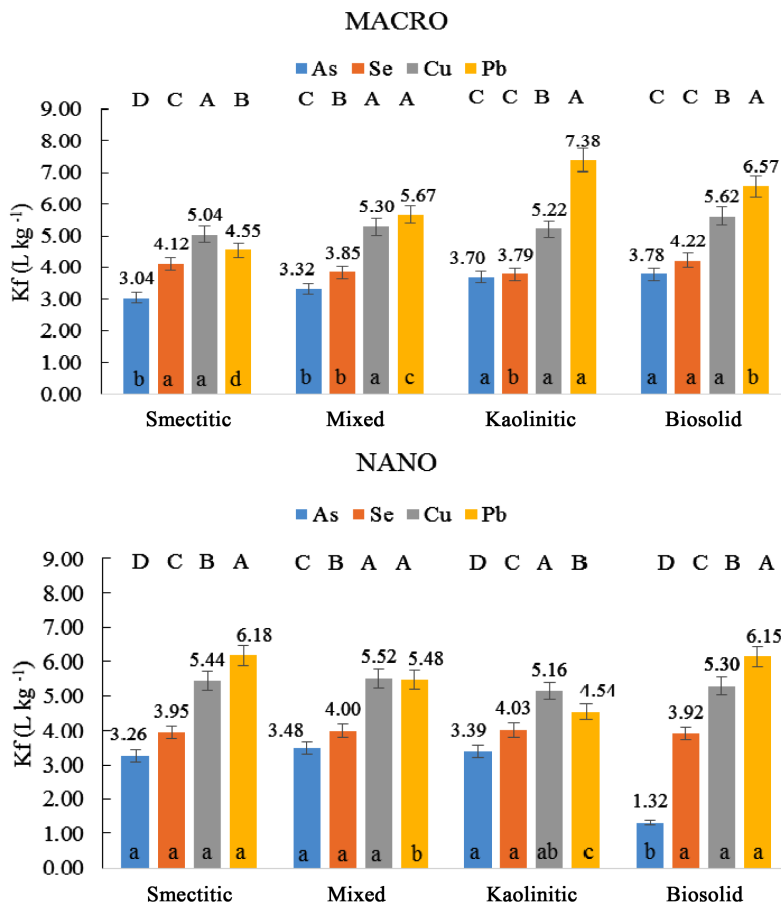


Figure 2. Multi-contaminant isotherm Kf values for As, Se, Cu, and Pb for macro- and nano-colloid fractions of different composition (capital letters portray trends across all four contaminants within each composition, while lower case letters display trends for each contaminant across all four compositions).

gle-contaminant isotherms. The alternating sorption affinities for Pb and Cu based on composition and size are consistent with conflicting sorption affinity exchanges reported for Cu and Pb in sediments, particularly in the presence of multiple contaminants [40]. Some studies suggest that preferential sorption of Pb over Cu occurs through inner sphere complexes due to its lower hydrolysis constant [22] [38], while others report preferential sorption of Cu over Pb due to its greater electronegativity and charge-to-radius ratio [41].

Conflicting preferential sorption trends for As and Se have also been reported in variable pH and anionic solution environments [18] [19] [28] [34]. Significant quantities of Cl⁻, NO₃⁻, PO₄³⁻, and SO₄²⁻ found in the kaolinitic and bio-nanocolloid fractions, may have offered significant competition for sorption of anions, and may have inhibited some cation sorption in the multi-contaminant isotherms. Additionally, sorption trends may have been influenced by Fe/Al and organic coatings as well as bridging effects between solution cations (natural or added contaminant) and anionic contaminants or enhanced aggregation caused by sorbed cation contaminants with free positive charge attracting negatively charged colloid particles. The later may cause encapsulation of some contaminants and deflect available sorption surfaces for others [5] [13] [20].

3.3. Anionic vs. Cationic Contaminants

Average Kf values for the anion (As and Se) and cation (Cu and Pb) contaminants for the single- and multi-contaminant isotherms demonstrated greater sorption affinities for cation-over anion-contaminants (Figure 3). This trend is consistent with other findings [12] [23] [25], and is likely due to the greater attraction of cations to the negatively charged colloid surfaces, as well as due to greater charge-to-radius ratios of Cu and Pb compared

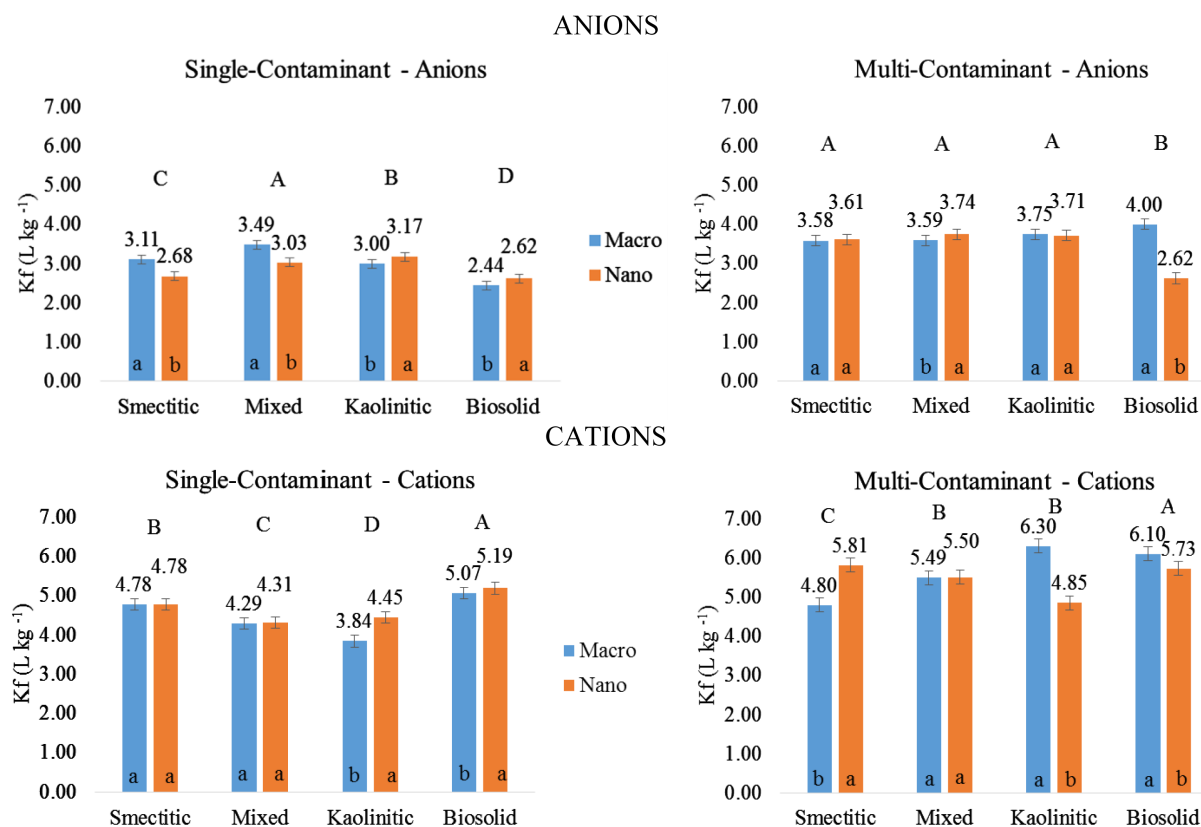


Figure 3. Average K_f values for anion-(As, Se) and cation-contaminants (Cu, Pb) determined from single- and multi-contaminant isotherms (capital letters portray trends based on composition, while lower case letters show significant differences based on size within each composition).

to As and Se [40]. Single-contaminant isotherms indicated the following sorption preference sequence based on composition for anionic contaminants: Mixed (A) > Kaolinitic (B) > Smectitic (C) > Biosolid (D). The multi-contaminant isotherms showed no significant sorption differences among the mineral colloids, but agreed with the single-contaminant isotherms by indicating greater overall affinities for anionic contaminants by mineral than bio-colloids (Figure 3). This is probably due to high concentrations of other anions in the bio-colloid fractions which may be out-competing the anionic contaminants for sorption sites [42]. Another likely explanation is the high negative/positive charge ratio of the bio-colloids inducing greater repulsion of the anionic contaminants [19] [43]. In contrast, both single- and multi-contaminant isotherms showed the bio-colloids having the strongest sorption affinity for both cationic contaminants (Figure 3). The sorption preference sequence for single-contaminant isotherms was: Biosolid (A) > Smectitic (B) > Mixed (C) > Kaolinitic (D), while for the multi-contaminant isotherms: Biosolid (A) > Mixed = Kaolinitic (B) > Smectitic (C). Sorption competition based on size showed mostly opposing trends between the single- and the multi-contaminant isotherms for both anion- and cation-contaminants (Figure 3). A comparison of average K_f values for anion- and cation-contaminant sorption regardless of colloid size and composition indicated significantly higher sorption affinities by multi- vs. single-contaminant isotherms. A similar comparison of average K_f values for all four contaminants suggested that smectitic and mixed nanocolloids can sorb significantly greater quantities of contaminants than corresponding macro-fractions while the opposite trend held true for the kaolinitic and biosolid colloids (Figure 3). Despite the fact that organic carbon and surface area have been shown in many studies to be key factors in understanding contaminant sorption patterns [12] [14] [32] [39], neither isotherm version (multi- or single-contaminant) gave consistent differences in size or composition-based trends when normalized to surface area and organic carbon content. Zeta potentials measured in the absence and presence of contaminants ($\alpha < 0.05$), ionic strength of contaminant added ($\alpha < 0.01$), contaminant type, OC, CEC and OC:SA were significant factors in the overall sorption model ($R^2 = 0.92$; $\alpha < 0.01$). The contradicting contaminant sorption trends for both cations and anions

highlight the complexities associated with predicting the behavior of colloids of various size and composition in a multi-contaminant natural environment.

3.4. Surface Sorption Characteristics

Single point zeta potential measurements were taken in the absence of contaminants and with additions of 2 and 10 mg·L⁻¹ mixed contaminants (Table 2) in order to decipher contaminant sorption mechanisms. In order to mimic natural conditions, the pH during the zeta potential measurements was not kept constant (Table 2), so that shifts in zeta potential are associated with pH and contaminant sorption changes through inner- or outer sphere attraction [14]. Zeta potentials without contaminants showed trends based on composition and size, with mineral nano-colloids exhibiting more negative values than corresponding macrocolloids (Table 2). Similarly, in the absence of contaminants all mineral colloid fractions showed more negative zeta potentials than the bio-colloid fractions (Table 2). The addition of contaminants caused significant shifts in zeta potential with opposing trends (positive vs. negative) for the mineral- and bio-colloid fractions, respectively. The large positive shift in zeta potential displayed by the smectitic macrocolloids and the mixed nano-colloids upon addition of contaminants indicates greater inner sphere cation contaminant attraction [14] (Table 2). Overall, the mineral colloid zeta potentials became more positive with the increased addition of contaminants, suggesting that the cations were out-competing the anions for inner sphere sorption (anions prefer outer sphere bonding and thus would have little to no effect on zeta potential values). Inner sphere bonding of Pb and Cu in the mineral colloid adsorption isotherm experiments was suggested through positive zeta potential shifts (Table 2) with increased contaminant loads ($\alpha = 0.05$) [14]. In contrast, outer sphere bonding was apparently the dominant sorption mechanism for the bio-colloids as indicated by negative zeta potential shifts (Table 2) with increased contaminant loads, suggesting a greater preference for anion contaminants. The pH drop with increasing contaminant loads shown by the mineral colloids also indicates inner sphere sorption [14]. Conversely, the prevalence of outer sphere bonding of the oxy-anion contaminants (As, Se) was indicated by increases in pH with increased contaminant loads. In single-contaminant isotherms the addition of anion contaminants increased the equilibrium solution pH by an average of 0.32 units over the initial pH, while the addition of cation contaminants caused a respective pH decrease of 0.31 units ($\alpha < 0.05$). The mixed macrocolloids showed the largest pH drop, while the bio-nanocolloids the largest increase with addition of contaminants, indicating prevalence of inner-sphere and outer-sphere bonding, respectively (Table 2).

4. Conclusions

The findings of this study demonstrate the complex characteristics of the competitive sorption behavior of natural colloid fractions of different sizes and compositions for As, Se, Cu, and Pb contaminants. It also emphasizes the potential shifting and even reversal of sorption trends predicted by different experimental approaches. Even though both single- and multi-contaminant isotherms suggested preferential sorption of cationic over anionic contaminants, sorption affinity estimates for each contaminant were greater by multi-contaminant isotherms and sorption sequences varied by composition and size. The varying and sometimes conflicting trends between mineralogical compositions and particle size were certainly affected by the presence of accessory minerals in the mixtures, surface OC and Fe/Al coatings, partial nano-aggregation phenomena, as well as the variable ionic composition of the solution environment. Zeta potential and pH changes after addition of different contaminant loads suggested mainly inner sphere bonding of cation contaminants to the nanocolloid surfaces and outer sphere bonding between oxy-anion contaminants and macro-colloid and bio-colloid surfaces.

These data also highlight the challenges posed by colloid heterogeneity (composition, size, surface characteristics) to predictions of contaminant interactions in natural environments and the importance of their comprehensive characterizations by water quality professionals and environmental consultants undertaking remediation tasks and by developers of engineered nanoparticles trying to model their environmental behavior.

References

- [1] McNaught, A.D. and Wilkinson, A. (1997) IUPAC Compendium of Chemical Terminology. 2nd Edition, Blackwell Science Publications, Oxford.
- [2] Christian, P., Von der Kammer, F., Baalousha, M. and Hofmann, T. (2008) Nanoparticles: Structure, Properties, Prep-

- aration and Behaviour in Environmental Media. *Ecotoxicology*, **17**, 326-343.
<http://dx.doi.org/10.1007/s10646-008-0213-1>
- [3] Maurice, P.A. and Hochella Jr., M.F. (2008) Nanoscale Particles and Processes: A New Dimension in Soil Science. *Advances in Agronomy*, **100**, 123-153. [http://dx.doi.org/10.1016/S0065-2113\(08\)00605-6](http://dx.doi.org/10.1016/S0065-2113(08)00605-6)
- [4] Theng, B.K.G. and Yuan, G.D. (2008) Nanoparticles in the Soil Environment. *Elements*, **4**, 395-399.
<http://dx.doi.org/10.2113/gselements.4.6.395>
- [5] Karathanasis, A.D. (2010) Composition and Transport Behavior of Soil Nanocolloids in Natural Porous Media. In: Frimmel, F.H. and NieBner, R., Eds., *Nanoparticles in the Water Cycle*, Chapter 4, Springer-Verlag, Berlin Heidelberg.
- [6] Tsao, T.M., Chen, Y.M. and Wang, M.K. (2011) Origin, Separation, and Identification of Environmental Nanoparticles: A Review. *Journal of Environmental Monitoring*, **13**, 1156-1163. <http://dx.doi.org/10.1039/c1em10013k>
- [7] Haering, K.C. and Evanylo, G.K. (2006) Mid-Atlantic Nutrient Management Handbook. CSREES Mid-Atlantic Regional Water Quality Program. MAWQP #06-02.
http://www.mawaterquality.org/capacity_building/ma_nutrient_mgmt_handbook.html
- [8] Lowry, G.V., Majetich, S., Matyjaszewski, K., Sholl, D. and Tilton, R. (2006) Transport, Targeting, and Applications of Metallic Functional Nanoparticles for Degredation of DNAPL Chlorinated Organic Solvents. Technical Report, Carnegie Mellon University, Pittsburgh. <http://dx.doi.org/10.2172/902659>
- [9] Unrine, J.M., Bertsch, P.M. and Hunyadi, S. (2008) Bioavailability, Trophic Transfer and Toxicity of Manufactured Metal and Metal Oxide Nanoparticles in Terrestrial Environments. In: Grassian, V.H., Ed., *Nanoscience and Nanotechnology Environmental and Health Impacts*, Chapter 14, John Wiley and Sons, Hoboken, 345-360.
<http://dx.doi.org/10.1002/9780470396612.ch14>
- [10] De Momi, A. and Lead, J.R. (2008) Behaviour of Environmental Aquatic Nanocolloids When Separated by Split-Flow Thin-Cell Fractionation (SPLITT). *Science of the Total Environment*, **405**, 317-323.
<http://dx.doi.org/10.1016/j.scitotenv.2008.05.032>
- [11] Bolea, E., Laborda, F. and Castillo, J.R. (2010) Metal Associations to Microparticles, Nanocolloids and Macromolecules in Compost Leachates: Size Characterization by Assymetrical Flow Field-Flow Fractionation Coupled to ICP-MS. *Analytica Chimica Acta*, **661**, 206-214. <http://dx.doi.org/10.1016/j.aca.2009.12.021>
- [12] Echeverría, J.C., Morera, M.T., Mazkiarán, C. and Garrido, J.J. (1998) Competitive Sorption of Heavy Metals by Soils. Isotherms and Fractional Factorial Experiments. *Environmental Pollution*, **101**, 275-284.
[http://dx.doi.org/10.1016/S0269-7491\(98\)00038-4](http://dx.doi.org/10.1016/S0269-7491(98)00038-4)
- [13] Cruz-Guzmán, M., Celis, R., Hermosin, M.C., Leone, P., Nègre, M. and Cornejo, J. (2003) Sorption-Desorption of Lead (II) and Mercury (II) by Model Associations of Soil Colloids. *Soil Science Society of America Journal*, **67**, 1378-1387. <http://dx.doi.org/10.2136/sssaj2003.1378>
- [14] Lair, G.J., Gerzabek, M.H., Haberhauer, G., Jakusch, M. and Kirchmann, H. (2006) Response of the Sorption Behavior of Cu, Cd, and Zn to Different Soil Management. *Journal of Plant Nutrition and Soil Science*, **169**, 60-68.
<http://dx.doi.org/10.1002/jpln.200521752>
- [15] Signes-Pastor, A., Burló, F., Mitra, K. and Carbonell-Barrachina, A.A. (2007) Arsenic Biogeochemistry as Affected by Phosphorus Fertilizer Addition, Redox Potential and pH in a West Bengal (India) Soil. *Geoderma*, **137**, 504-510.
<http://dx.doi.org/10.1016/j.geoderma.2006.10.012>
- [16] Su, C. and Suarez, D.L. (2000) Selenate and Selenite Sorption on Iron Oxides: An Infrared and Electrophoretic Study. *Soil Science Society of America Journal*, **64**, 101-111. <http://dx.doi.org/10.2136/sssaj2000.641101x>
- [17] Covelo, E.F., Vega, F.A. and Andrade, M.L. (2007) Competitive Sorption and Desorption of Heavy Metals by Individual Soil Components. *Journal of Hazardous Materials*, **140**, 308-315.
<http://dx.doi.org/10.1016/j.jhazmat.2006.09.018>
- [18] Gao, X. (2008) Speciation and Geochemical Cycling of Lead, Arsenic, Chromium, and Cadmium in a Metal-Contaminated Histosol. Doctoral Dissertation, ProQuest Dissertations and Thesis, Accession Order No. 3294674.
- [19] Violante, A. (2013) Chapter Three: Elucidating Mechanisms of Competitive Sorption at the Mineral/Water Interface. In: Donald, L.S., Ed., *Advances in Agronomy*, Academic Press, Waltham, 111-176.
- [20] Redman, A.D., Macalady, D.L. and Ahmann, D. (2002) Natural Organic Matter Affects Arsenic Speciation and Sorption onto Hematite. *Environmental Science & Technology*, **36**, 2889-2896. <http://dx.doi.org/10.1021/es0112801>
- [21] Saada, A.D., Breeze, D., Crouzet, C., Cornu, S. and Baranger, P. (2003) Adsorption of Arsenic (V) on Kaolinite and on Kaolinite-Humic Acid Complexes: Role of Humic Acid Nitrogen Groups. *Chemosphere*, **51**, 757-763.
[http://dx.doi.org/10.1016/S0045-6535\(03\)00219-4](http://dx.doi.org/10.1016/S0045-6535(03)00219-4)
- [22] Heidmann, I., Christl, I., Leu, C. and Kretzschmar, R. (2005) Sorption of Cu and Pb to Kaolinite-Fulvic Acid Colloids:

- Assessment of Sorbent Interactions. *Geochimica et Cosmochimica Acta*, **69**, 1675-1686.
<http://dx.doi.org/10.1016/j.gca.2004.10.002>
- [23] Karathanasis, A.D., Johnson, D.M.C. and Matocha, C.J. (2005) Biosolid Colloid-Mediated Transport of Copper, Zinc, and Lead in Waste-Amended Soils. *Journal of Environmental Quality*, **34**, 1153-1164.
<http://dx.doi.org/10.2134/jeq2004.0403>
- [24] Essington, M.E. (2004) *Soil and Water Chemistry: An Integrative Approach*. CRC Press LLC., Boca Raton.
- [25] Smith, E., Naidu, R. and Alston, A.M. (2002) Chemistry of Inorganic Arsenic in Soils: II. Effect of Phosphorus, Sodium, and Calcium on Arsenic Sorption. *Journal of Environmental Quality*, **31**, 557-563.
<http://dx.doi.org/10.2134/jeq2002.0557>
- [26] Bowell, R.J. (1994) Sorption of Arsenic by Iron Oxides and Oxyhydroxides in Soils. *Applied Geochemistry*, **9**, 279-286.
[http://dx.doi.org/10.1016/0883-2927\(94\)90038-8](http://dx.doi.org/10.1016/0883-2927(94)90038-8)
- [27] Balasoiu, C.F., Zagury, G.J. and Deschênes, L. (2001) Partitioning and Speciation of Chromium, Copper, and Arsenic in CCA-Contaminated Soils: Influence of Soil Composition. *Science of the Total Environment*, **280**, 239-255.
[http://dx.doi.org/10.1016/S0048-9697\(01\)00833-6](http://dx.doi.org/10.1016/S0048-9697(01)00833-6)
- [28] Lui, F., De Cristofaro, A. and Violante, A. (2001) Effect of pH, Phosphate and Oxalate on the Adsorption, Desorption of Arsenate on/from Goethite. *Soil Science*, **166**, 197-208. <http://dx.doi.org/10.1097/00010694-200103000-00005>
- [29] Huang, P.M. (1975) Retention of Arsenic by Hydroxy-Aluminum on Surfaces of Micaceous Mineral Colloids. *Soil Science Society of America Journal*, **39**, 271-274. <http://dx.doi.org/10.2136/sssaj1975.03615995003900020016x>
- [30] Bar-Yosef, B. and Meek, D. (1987) Selenium Sorption by Kaolinite and Montmorillonite. *Soil Science*, **144**, 11-19.
<http://dx.doi.org/10.1097/00010694-198707000-00003>
- [31] Goldberg, S. (2013) Modeling Selenite Adsorption Envelopes on Oxides, Clay Minerals, and Soils Using the Triple Layer Model. *Soil Science Society of America Journal*, **77**, 64-71. <http://dx.doi.org/10.2136/sssaj2012.0205>
- [32] Peak, D. and Sparks, D.L. (2002) Mechanisms of Selenate Adsorption on Iron Oxides and Hydroxides. *Environmental Science & Technology*, **36**, 1460-1466. <http://dx.doi.org/10.1021/es0156643>
- [33] Waychunas, G.A., Kim, C.S. and Banfield, J.A. (2005) Nanoparticulate Iron Oxide Minerals in Soils and Sediments: Unique Properties and Contaminant Scavenging Mechanisms. *Journal of Nanoparticle Research*, **7**, 409-433.
<http://dx.doi.org/10.1007/s11051-005-6931-x>
- [34] Goh, K. and Lim, T. (2004) Geochemistry of Inorganic Arsenic and Selenium in a Tropical Soil: Effect of Reaction Time, pH, and Competitive Anions on Arsenic and Selenium Adsorption. *Chemosphere*, **55**, 849-859.
<http://dx.doi.org/10.1016/j.chemosphere.2003.11.041>
- [35] Jackson, B.P. and Miller, W.P. (1999) Soluble Arsenic and Selenium Species in Fly Ash/Organic Waste-Amended Soils Using Ion Chromatography-Inductively Coupled Plasma Mass Spectrometry. *Environmental Science & Technology*, **33**, 270-275. <http://dx.doi.org/10.1021/es980409c>
- [36] Donner, E., Ryan, C.G., Howard, D.L., Zarcinas, B., Scheckel, K.G., McGrath, S.P., *et al.* (2012) A Multi-Technique Investigation of Copper and Zinc Distribution, Speciation and Potential Bioavailability in Biosolids. *Environmental Pollution*, **166**, 57-64. <http://dx.doi.org/10.1016/j.envpol.2012.02.012>
- [37] Strawn, D.G., Palmer, N.E., Furnare, L.J., Goodell, C. and Amonette, J.E. (2004) Copper Sorption Mechanisms on Smectites. *Clays and Clay Minerals*, **52**, 321-333. <http://dx.doi.org/10.1346/CCMN.2004.0520307>
- [38] Sipos, P., Németh, T., Kis, V.K. and Mohai, I. (2008) Sorption of Copper, Zinc and Lead on Soil Mineral Phases. *Chemosphere*, **73**, 461-469. <http://dx.doi.org/10.1016/j.chemosphere.2008.06.046>
- [39] Morton, J.D., Semrau, J.D. and Hayes, K.F. (2001) An X-Ray Absorption Spectroscopy Study of the Structure and Reversibility of Copper Adsorbed to Montmorillonite Clay. *Geochimica et Cosmochimica Acta*, **65**, 2709-2722.
[http://dx.doi.org/10.1016/S0016-7037\(01\)00633-0](http://dx.doi.org/10.1016/S0016-7037(01)00633-0)
- [40] Seo, D.C., Yu, K. and DeLaune, R.D. (2008) Comparison of Monometal and Multimetal Adsorption in Mississippi River Alluvial Wetland Sediment: Batch and Column Experiments. *Chemosphere*, **73**, 1757-1764.
<http://dx.doi.org/10.1016/j.chemosphere.2008.09.003>
- [41] Selim, H.M. (2012) *Competitive Sorption and Transport of Heavy Metals in Soils and Geological Media*. CRC Press, Boca Raton, 426. <http://dx.doi.org/10.1201/b13041>
- [42] Goldberg, S. and Glaubig, R.A. (1987) Effect of Saturating Cation, pH, and Aluminum and Iron Oxides on the Flocculation of Kaolinite and Montmorillonite. *Clays and Clay Minerals*, **35**, 220-227.
<http://dx.doi.org/10.1346/CCMN.1987.0350308>
- [43] Shen, Y.H. (1999) Sorption of Humic Acid to Soil: The Role of Mineralogical Composition. *Chemosphere*, **38**, 2489-2499. [http://dx.doi.org/10.1016/S0045-6535\(98\)00455-X](http://dx.doi.org/10.1016/S0045-6535(98)00455-X)

Scientific Research Publishing (SCIRP) is one of the largest Open Access journal publishers. It is currently publishing more than 200 open access, online, peer-reviewed journals covering a wide range of academic disciplines. SCIRP serves the worldwide academic communities and contributes to the progress and application of science with its publication.

Other selected journals from SCIRP are listed as below. Submit your manuscript to us via either submit@scirp.org or [Online Submission Portal](#).

